Vol. 35. No. 1 (2013) 84-94

Tribology in Industry

www.tribology.fink.rs

RESEARCH

Effect of Contact Temperature Rise During Sliding on the Wear Resistance of TiNi Shape Memory Alloys

S.K. Roy Chowdhury[a], K. Malhotra[a], H. Padmawar[a]

[a]*Department of Mechanical Engineering, Indian Institute of Technology, Kharagpur 721 302, India.*

Keywords:

TiNi alloy
Wear resistance
Phase transformation
Contact temperature
Pseudoelasticity

Corresponding Author:

S.K. Roy Chowdhury
Professor
Department of Mechanical Engineering, Indian Institute of Technology, Kharagpur 721 302, India
E-mail: skrc@mech.iitkgp.ernet.in

A B S T R A C T

The high wear resistance of TiNi shape memory alloys has generally been attributed to its pseudoelastic nature. In the present work the hardening effect due to its phase transformation from martensite to austenite due to frictional heating during sliding has been considered. Based on existing constitutive models that represent the experimental results of TiNi shape memory alloys a theoretical model of the dependence of wear-resistance on the contact temperature rise has been developed.

The analysis was further extended to include the operating and surface roughness parameters. The model essentially indicates that for these alloys wear decreases with the rise in contact temperature over a wide range of load, speed and surface roughness combination during sliding. This means that the wear resistance of these alloys results from the very cause that is normally responsible for the increased wear and seizure of common engineering materials.

Preliminary wear tests were carried out with TiNi alloys at varying ambient temperature and varying load-speed combinations and the results agree well with the theoretical predictions.

1. INTRODUCTION

Titanium-Nickel (TiNi) alloys are widely known for their shape memory effect and pseudoelasticity. These effects are due to the fact that these alloys can exist in two different temperature-dependent crystal structures: martensite at low temperatures and austenite at high temperatures. When a TiNi alloy in martensite phase is heated the phase changes to austenite and if it is cooled after complete transformation it reverts back to martensite phase with some hysteresis. The phase transformation can also be induced by change in stress level and the initial phase can be recovered with the removal of the stress. Here a decrease in stress is equivalent to increase in temperature resulting in nucleation of martensite. This gives rise to basically three different forms from the practical application point of view: martensite, stress induced martensite and austenite. In the martensitic form the material is soft and ductile and can be easily deformed. In the stress induced martensitic form it is highly elastic and it can return to its original shape on unloading even after substantial deformation. This form is known

as pseudoelasticity. In the austenitic form it is strong and hard [1,2].

A good deal of research has been carried out on the shape memory effect of TiNi alloys and their applications [3-8]. These alloys have also been found to be extremely resistant to wear in sliding, fatigue, abrasion and erosion modes [9-14]. Some Ti based alloys have also been widely used in biomedical engineering [15]. The high wear resistance of TiNi alloys has generally been attributed not to the increase in hardness but to the pseudoelastic nature of the alloys. The argument here is that in the pseudoelastic state, contact between the sliding pair would be largely elastic and wear is likely to be small since in pseudoelastcity recoverable strain may reach up to 8% or more [16]. Li [10] proposed that the excellent wear resistance of these alloys is influenced by their hardness too. According to this proposition wear resistance is partly influenced by pseudoelasticity and partly by hardness depending on the material state. High hardness contributes to wear resistance when the pseudoelasticity is of low order. Some authors attributed the wear resistance of TiNi alloys to causes other than pseudoelasticity, for example, work hardening [17], erosion resistance [18]. Abedini et al. [19] observed decrease in wear with the increase in temperature and attributed this effect to both pseudoelasticity and higher strength of the alloy in the austenitic state at higher temperatures. Some attempts have been made to develop a model that shows increase in hardness of these alloys with the increase in temperature in micro level [20].

However the effect of frictional heat generated at the contact area between a sliding pair on the wear resistance of these alloys has not been considered hitherto. The present work explores the possibility of attributing wear resistance of TiNi alloys to the hardening effect due to phase transformation from martensite to austenite due to contact temperature rise during sliding. The deformation during wear process is mostly not recoverable and therefore it is likely that the wear resistance would be more influenced by hardness than pseudoelasticity that occurs in a narrow temperature zone near the austenitic transformation temperature. In tribological contacts the temperature rise due to frictional heat generated at the peaks of the asperities can be of very high order of magnitude and under normal circumstances for most engineering materials this has an adverse effect on the life of rubbing components due to increased wear and friction. If, however, the wear resistance of near equi-atomic TiNi alloys is indeed due to hardening during the martensite to austenite phase transformation due to frictional heat then this would mean that the wear resistance of these alloys results from the very cause that is normally responsible for the increased wear and seizure of engineering components.

The paper attempts to develop a simple theoretical model to relate contact temperature rise during sliding and wear resistance of TiNi alloys in the macroscopic level. Some elementary experiments were also carried out in support of the theoretical predictions.

2. A THEORETICAL MODEL OF TEMPERATURE DEPENDENCE OF HARDNESS AND WEAR RESISTANCE OF TiNi ALLOYS

In order to develop a theoretical model we first consider a 1-D constitutive model that represents the existing experimental results of TiNi shape memory alloys. Several such models exist and they all basically couple a phenomenological macro-scale constitutive law relating stress to strain temperature and phase fraction with a kinetic law that describes the evolution of the phase fraction as a function of stress and temperature [8,21,22]. Here we use the model proposed by Liang and Rogers [8].

In a typical martensitic phase change as a function of temperature there are four important temperatures: martensitic start temperature (M_s), martensitic finish temperature (M_f), austenitic start temperature (A_s) and austenitic finish temperature (A_f). Liang and Rogers [8] described the martensitic fraction (ξ) vs. temperature (T) relation as a cosine function for a shape memory alloy where $A_s > M_s$ and the equation describing the phase transformation is given as:

$$\underset{M\to A}{\xi} = \frac{1}{2}[\cos\{a_A(T - A_S)\} + 1] \qquad (1)$$

where ξ is the martensite volume fraction, T is the alloy specimen temperature and the constant a_A is given by:

$$a_A = \pi/(A_f - A_s) \quad (2)$$

Since we are interested in the hardening effect of the shape memory alloys with rise in contact temperature only the phase transformation between martensite to austenite needs to be considered. It has been shown [8] that the phase changes temperatures are linearly related to the applied stress and within the range between austenite start and finish temperatures we may write:

$$\frac{\sigma'}{C} = A_0 - A_s^0 \quad (3)$$

where A^0_s is the austenite start temperatures in stress free state and C is a constant. Combining equations (1) and (3) we have:

$$\underset{M\to A}{\xi} = \frac{1}{2}[\cos(a_A(T - \frac{\sigma'}{C} - A_s^o)) + 1] \quad (4)$$

Here a_A will change to:

$$a_A = C\pi/(A_f^0 - A_s^0)$$

A_f^0 being the austenite finish temperature in stress free state. Since in the present case we consider that the phase transformation will be complete when all the martensite changes into austenite we may set $\underset{M-A}{\xi}$ to zero and this gives:

$$\underset{M\to A}{\sigma'} = C(T - \frac{\pi}{a_A} - A_s^o) \quad (5)$$

In many cases hardness is taken as three times the yield stress and therefore the temperature dependent hardness variation during martensite to austenite transformation can be given by:

$$\underset{M\to A}{H} = 3C[T - \frac{\pi}{a_A} - A_s^o] \quad (6)$$

Here C, A_s^o and a_A are all constants and therefore hardness varies only with temperature. In general in sliding wear hardness plays an important role and this is given by Archard's wear law:

$$V = K_w \frac{Wx}{\underset{M\to A}{H}} \quad (7)$$

Here K_w is the wear coefficient, W is the load, x the sliding distance and H the hardness of the softer of the two rubbing materials. Combining equations (6) and (7) a simple temperature dependent wear equation can be written as:

$$V = \frac{K_w Wx}{3C(T - B)} \quad (8)$$

where $B = (A_s^o + \frac{\pi}{a_A})$.

Defining non-dimensional wear volume $\bar{V}$ and non-dimensional temperature $\bar{T}$ as:

$$\bar{V} = \frac{V}{Wx/CB} \quad \text{and} \quad \bar{T} = \frac{T}{B}$$

we may rewrite equation (8) in non-dimensional form as:

$$\bar{V} = \frac{K_w}{3(\bar{T} - 1)} \quad (9)$$

Variation of non-dimensional wear with non-dimensional temperature with the experimental value of K_w from section-5(b) is shown in Fig. 1.

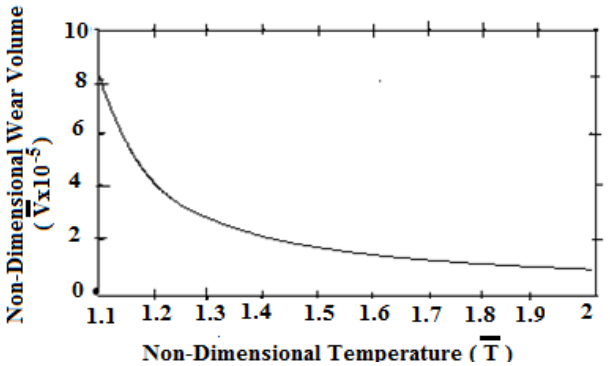

Fig. 1. Variation of non-dimensional wear with non-dimensional temperature with the average K_w value of 2.5E-5 from the experimental results in section 5 (b).

Clearly this shows decrease in wear with increase in temperature and this supports the argument that with the increase in contact temperature is likely to cause the austenitic phase transformation of TiNi alloy leading to increased wear resistance due to increase in hardness.

3. INFLUENCE OF TRIBOLOGICAL OPERATING AND MATERIAL PARMETERS THAT AFFECT CONTACT TEMPERATURE RISE

The total contact temperature at the sliding interface is the sum of the bulk temperature T_{bulk} and the contact temperature rise θ.

$$T=\theta+T_{bulk} \tag{10}$$

In general T_{bulk} may be taken as atmospheric temperature and therefore the effective temperature at the sliding interface is mainly dominated by the contact temperature rise θ. The contact temperature rise between sliding bodies has been researched widely ever since Block [23] and Jaeger [24] reported their pioneering works on flash temperature in 1937 and 1942 respectively. Subsequently, Archard [25] proposed the following set of handy equations to predict the mean contact temperature rise for different speed and deformation conditions:

$$\begin{aligned}
\theta_{mhe} &= 0.41\mu\left[\frac{WvE^*}{K\rho cR}\right]^{1/2} \\
\theta_{mhp} &= 0.8\frac{\mu H^{3/4}}{(K\rho c)^{1/2}}W^{1/4}v^{1/2} \\
\theta_{mle} &= 0.142\mu\frac{W^{2/3}E^{*1/3}v}{KR^{1/3}} \\
\theta_{mlp} &= 0.125\mu\frac{W^{1/2}v(\pi H)^{1/2}}{K}
\end{aligned} \tag{11}$$

Here mhe, mhp ,mle and mlp indicate mean high speed elastic, mean high speed plastic, mean low speed elastic and mean low speed plastic respectively and v is the sliding speed, E^* the equivalent elastic modulus, K the thermal conductivity, ρ the density, c specific heat and R the protrusion radius. These equations are widely used even today for their simplicity even though they essentially refer to continuous area of contact and disregard the discrete nature of rough surfaces. The deformation conditions for rough surfaces with typically Gaussian distribution of surface heights are ideally determined using the plasticity index (ψ) given by:

$$\psi=\frac{E^*}{H}\sqrt{\frac{\sigma}{r}} \tag{12}$$

where the equivalent elasticity modulus E^* is given by $\frac{1}{E^*}=\frac{1-\upsilon^2}{E_1}+\frac{1-\upsilon^2}{E_2}$, σ is the standard deviation of the surface height distribution and r is the asperity radius. A contact is considered to be elastic if ψ< 0.6 and plastic if ψ > 1.5. Speed criterion (L) is given by:

$$L = va\rho c/2K \tag{13}$$

where a is the contact radius. A contact is considered to be fast if L > 5 and slow if L < 0.5. However, since Archard's contact temperature formulations are essentially for single contact area we consider the bulk deformation and therefore we would consider the deformation to be plastic if $P/(\pi a^2) > H$. Taking T≈θ and combining equations (8) and (11) we may write the wear volumes for different speed and deformation conditions in terms of operating and material parameters in non-dimensional form as:

$$\begin{aligned}
\bar{V}_{mhe} &= \frac{K_w}{3(0.41\mu\bar{W}^{1/2}\bar{v}_e^{-1/2}-1)} \\
\bar{V}_{mpe} &= \frac{K_w}{3(0.8\mu\bar{H}^{1/4}\bar{W}^{1/4}\bar{v}_p^{-1/2}-1)} \\
\bar{V}_{mle} &= \frac{K_w}{3(0.142\mu\bar{E}^{-2/3}\bar{W}^{2/3}\bar{v}_e-1)} \\
\bar{V}_{mlp} &= \frac{K_w}{3(0.125\mu\bar{H}^{-1/2}\bar{W}^{1/2}\bar{v}_p-1)}
\end{aligned} \tag{14}$$

where non-dimensional wear volume $\bar{V}$, non-dimensional load $\bar{W}$, non-dimensional velocity in elastic case $\bar{v}_e$, non-dimensional velocity in plastic case $\bar{v}_p$, non-dimensional elastic modulus $\bar{E}$ and non-dimensional hardness $\bar{H}$ are given by :

$$\bar{V}=\frac{VCB}{Wx};\ \bar{W}=\frac{K_w}{B\rho CR^2};\ \bar{v}_e=\frac{v}{(BK/E^*R)};$$

$$\bar{v}_p=\frac{v}{(BK/HR)};\ \bar{E}=\frac{E^*}{B\rho C};\ \bar{H}=\frac{H}{B\rho C}$$

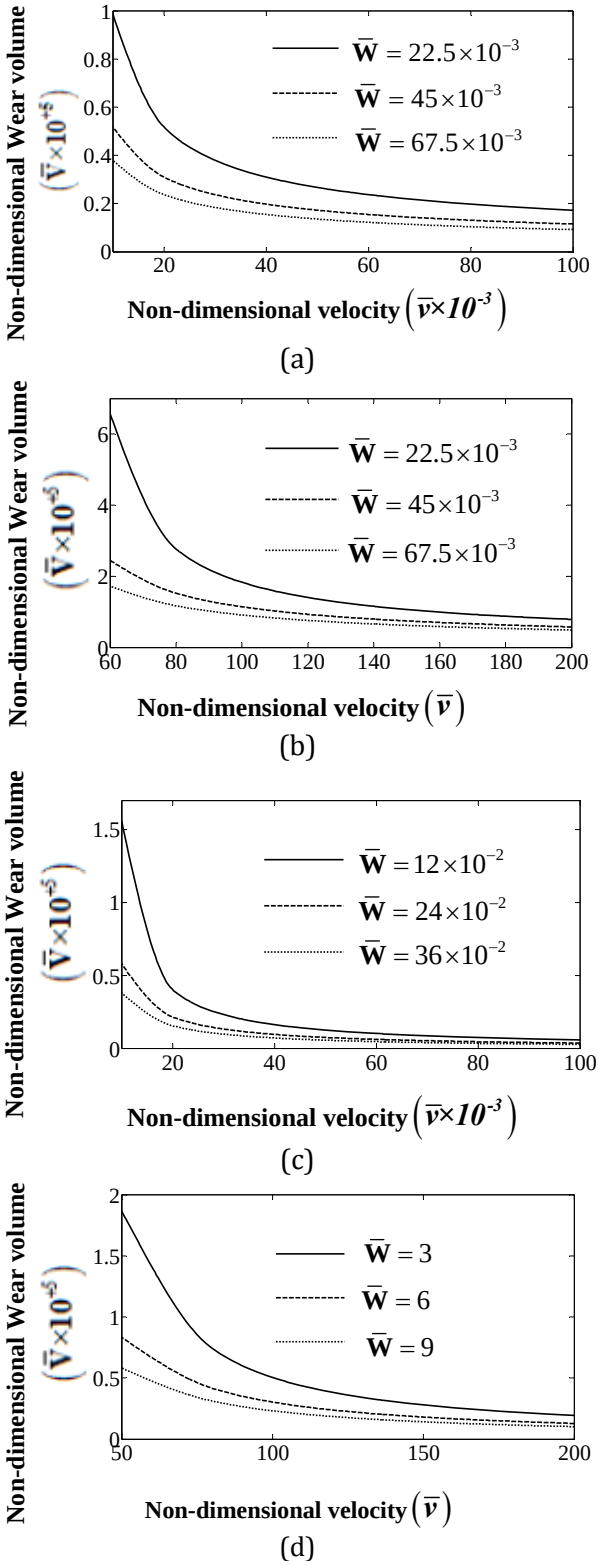

Fig. 2. Plots of non-dimensional wear against non-dimensional velocity for (a)High Speed Elastic (b) High Speed Plastic (c) Low Speed Elastic (d) Low Speed plastic contacts over a range of non-dimensional load with experimental value of K_w =2.5E-5 and μ =0.3, $\overline{E}$ =555 and $\overline{H}$ =6.

Non-dimensional wear calculated with the average value of experimental wear coefficient from section-5(b) plotted against non-dimensional velocity over a range of non-dimensional load for different speed and load conditions are shown in Fig. 2.

4. INFLUENCE OF SURFACE ROUGHNESS PARAMETERS THAT AFFECT CONTACT TEMPERATURE RISE.

A good deal of work [26-29] has also been carried out to include the multiple heat inputs in contact temperature analysis. Based on Archard's model a set of equations that takes into account the surface roughness parameters for both Gaussian and exponential distributions of surface heights can be written [29]. The average flash temperature equations in terms of material and roughness parameters and with exponential surface height distributions may be given by:

$$\theta_{av.he}=1.149\frac{\mu EV^{1/2}}{(K\rho C)^{1/2}}\frac{\sigma^{3/4}}{r^{1/4}}$$
$$\theta_{av.hp}=1.72\frac{\mu HV^{1/2}}{(K\rho C)^{1/2}}\sigma^{1/4}r^{1/4}. \qquad (15)$$
$$\theta_{av.le}=0.368\frac{\mu EV}{K}\sigma$$
$$\theta_{av.lp}=0.5\frac{\mu VH}{K}r^{1/2}\sigma^{1/2}$$

Since exponential distribution represents the upper reaches of the asperities this may be used as a first approximation. There are at least two issues which need to be addressed here. Firstly, from operating conditions and other considerations we need to identify the equation among the four that needs to be used in a particular application. This can be determined using equations (12) and (13) for rough surfaces and for single contact elementary plasticity condition $P/(\pi a^2) > H$ may be used.The other important issue is that the contact temperatures in equation (15) appear to be independent of load but depends on the roughness parameters σ and r. The explanation lies in the fact that the total real area of contact per unit area A_r, total elastic load per unit area W_e and total plastic load per unit area W_p are given by [30]:

$$A_r = N\int_d^{\infty} \pi a^2 \varphi(z) dz = 2\pi r n \sigma \qquad (16)$$

$$W_e = 0.8 A_r E^* (\sigma / r)^{1/2} \qquad (17)$$

$$W_p = 2\pi r n H \sigma \qquad (18)$$

Here N is the total number of asperities per unit area, φ(z) is the surface height distribution, n number of asperities in contact , A_r is the real area of contact. This clearly shows the dependence of load on real area of contact which in turn depends on the roughness parameters σ and r. Now combining equations (8), (15) and the non-dimensional scheme used in equation(14) we may write the wear volumes for different speed and deformation conditions in terms of operating and material parameters in non-dimensional form as:

$$\bar{V}_{avhe} = \frac{K_w}{3(1.149\mu \bar{v}^{1/2} \bar{E}^{-1/2} \bar{\sigma}^{3/4} - 1)}$$

$$\bar{V}_{avhp} = \frac{K_w}{3(1.72\mu \bar{v}^{-1/2} \bar{H}^{-1/2} \bar{\sigma}^{3/4} - 1)}$$

$$\bar{V}_{avle} = \frac{K_w}{3(0.368\mu \bar{v} \bar{\sigma} - 1)} \qquad (19)$$

$$\bar{V}_{avlp} = \frac{K_w}{3(0.5\mu \bar{v}^{1/2} \bar{\sigma}^{1/2} - 1)}$$

where $\bar{\sigma} = \frac{\sigma}{r}$.

Non-dimensional wear calculated with the average value of the wear-coefficient from section-5(b) plotted against non-dimensional roughness over a range of non-dimensional load for different load and speed conditions are shown in Fig. 3.

Figs. 2 and 3 essentially show that the wear decreases with the increase in velocity over a range of load and with the increase in roughness over a range of velocity. This in turn indicates that wear decreases with contact temperature and clearly this is because, contrary to the behaviour of normal engineering materials hardness of this class of TiNi alloys increases with contact temperature rise.

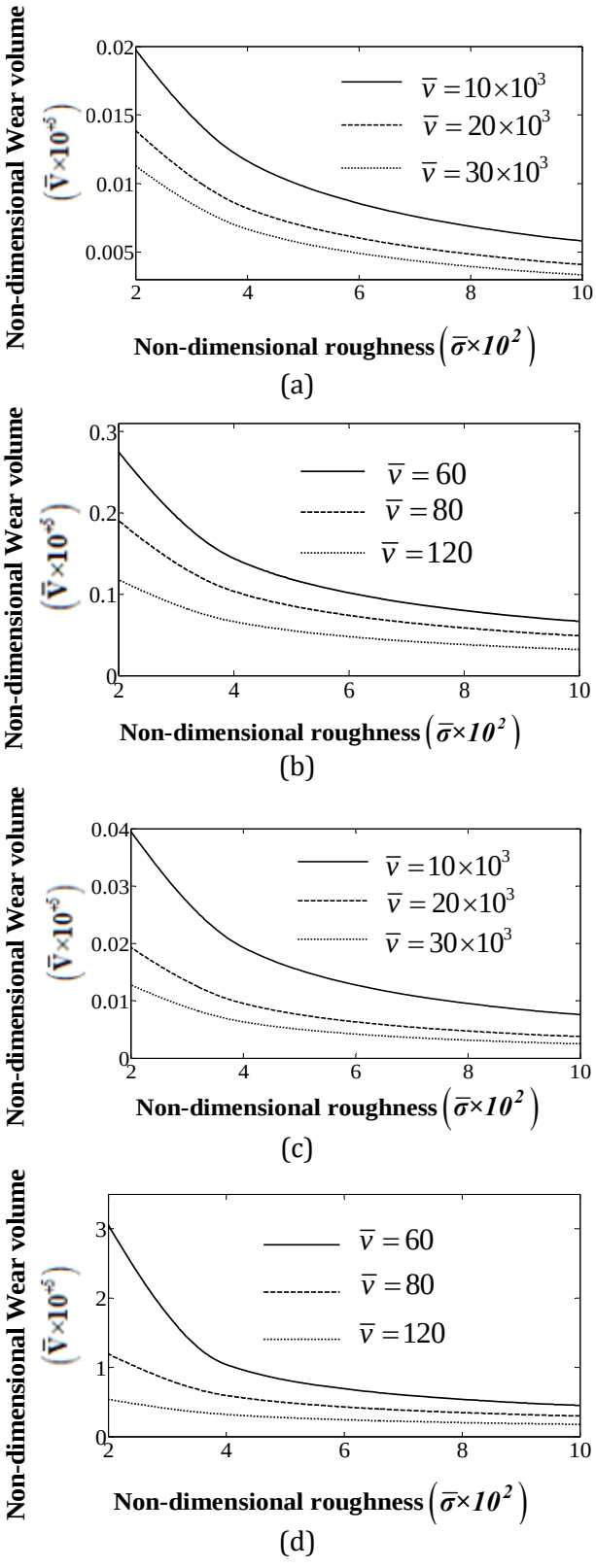

Fig. 3. Plots of non-dimensional wear against non-dimensional roughness for (a)High speed Elastic (b) High speed Plastic (c) Low speed Elastic (d) Low speed plastic contacts over a range of non-dimensional load with experimental value of K_w =2.5E-5 and μ =0.3, $\bar{E}$ =555 and $\bar{H}$ =6.

5. EXPERIMENTAL DETAILS

Two preliminary sliding wear tests were carried out with TiNi alloys one at a constant load and speed but at varying specimen temperature and the other at a constant load and ambient temperature but at varying sliding speed.

(a) Sliding wear test with TiNi alloy at a constant load and speed but at varying specimen temperature.

This set of tests was aimed at determining the dependence of wear resistance of these alloys on specimen temperature. A near equi-atomic TiNi (Ti-51at-%Ni) alloy was prepared in a vacuum induction melting furnace. A disc specimen of 42mm diameter and 10mm thickness was then prepared with the alloy. Wear tests were carried out in a commercially available high-temperature, high-vacuum Tribometer, initially using a 10 mm diameter tungsten carbide ball rubbing against the alloy disc at a normal load of 1.1 kg and a disc rotational speed of 200 rpm for 300 seconds in water media. Tungsten carbide balls of relatively high hardness were chosen so that the wear characteristics of the alloy disc alone could be observed. The water temperature was varied between 20 ^{0}C to 80 ^{0}C in order to obtain different specimen temperatures. The weight loss of the specimen was measured using a high precision balance. The results with the tungsten carbide balls are shown in Fig. 4.

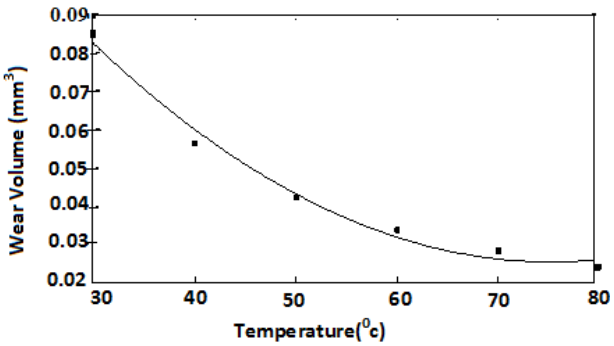

Fig. 4. Plot of wear volume of a TiNi alloy disc, rubbing against a tungsten carbide ball, against the specimen temperature.

(b) Sliding wear test of TiNi alloy at a constant load and ambient temperature but at varying sliding speed.

Another TiNi (Ti-51at-%Ni) specimen was prepared following similar procedure and sliding tests were carried out using the same Tribometer, a steel pin of 5mm radius pressed against the TiNi alloy disc specimen under a constant normal load of 5 N and at varying sliding speeds of 20 mm/s, 40 mm/s, 80 mm/s and 150 mm/s so that different contact temperatures could be generated. The contact temperatures for each load and speed combination were calculated using Archard's flash temperature equations, reproduced in a convenient form in equation (10). The deformation conditions were determined using the elementary plasticity condition $P/(\pi a^2) > H$, a being the contact radius. The speed conditions were determined using equation (13). With these constraints all the test conditions turned out to be high speed elastic. The weight loss of the specimen was again measured using a high precision balance and the plot of experimental wear volume against calculated specimen temperature is shown in Fig. 5.

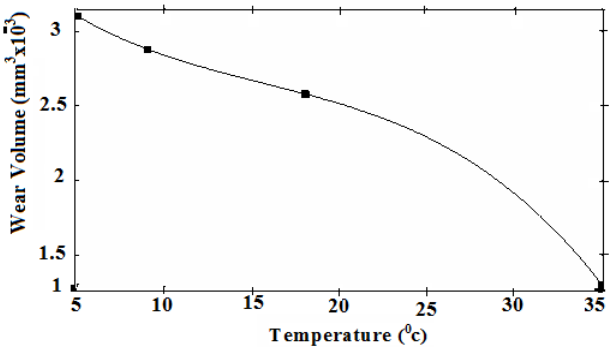

Fig. 5. A plot of wear volume against contact temperature during sliding experiments with TiNi alloy disc pressed against a steel pin at a normal load of 5N and different sliding speeds.

It can be seen that the trend of wear vs. temperature plots in Fig. 4 for tests under constant load and speed but at varying specimen temperature is similar to this plot. This supports our argument that the rise in contact temperature during sliding due to frictional heat itself may be sufficient to cause the initial martensite to austenite phase transformation and the associated increase in hardness that leads to decrease in wear with increasing sliding velocity.

It is now necessary to consider the phase transformation due to the frictional heat generated during the sliding process. The X-ray diffraction signatures of the sample in the constant load and speed test were recorded before and

after the wear test. The signature of the initial unworn surface is shown in Fig. 6. This indicates rhombohedral and monoclinic crystal structures which indicate the presence of martensite phase. Presence of some Ni_4Ti_3 was also observed. This may be due to the presence of excess Ni while preparing the sample. In general formation of Ni_4Ti_3 is favoured in case of excess aging of sample but in the present case no excess aging was done and therefore this cannot be the reason for its presence. The X-ray analysis of the worn surface is shown in Fig. 7 and this indicates cubic crystal structure which is responsible for the highest peak. Cubic crystal structure indicates the presence of austenite phase in worn surface. The analysis also indicates the presence of small amount of TiO_2 and this may partly contribute to the wear resistance of TiNi alloy as suggested by Korshunov [31].

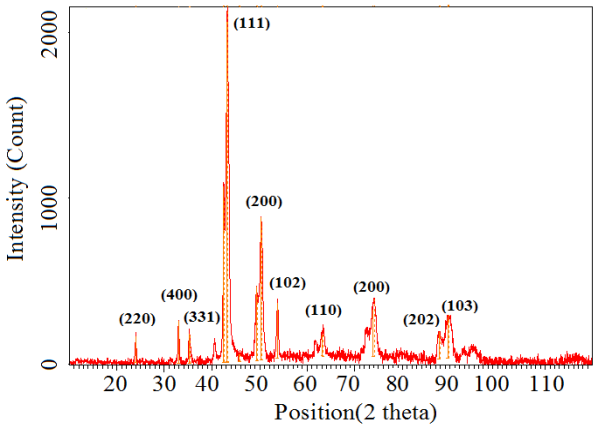

Fig. 6. X-ray diffraction signature of the initial surface of TiNi alloy.

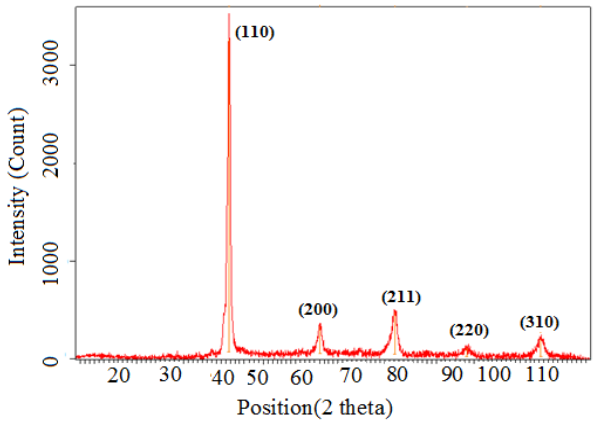

Fig. 7. X-ray diffraction signature of the worn surface of TiNi alloy.

SEM micrograph of the worn surface is shown in Fig. 8. The micrograph generally indicates fatigue fracture in the worn surface. In the presence of high elastic stresses in austenitic or pseudoelastic state repeated cyclic loading during sliding may introduce surface or subsurface cracks that eventually lead to formation of large cracks on the surface as seen in Fig. 8. Severe plastic deformation needed for ploughing wear in martensitic state could not be detected.

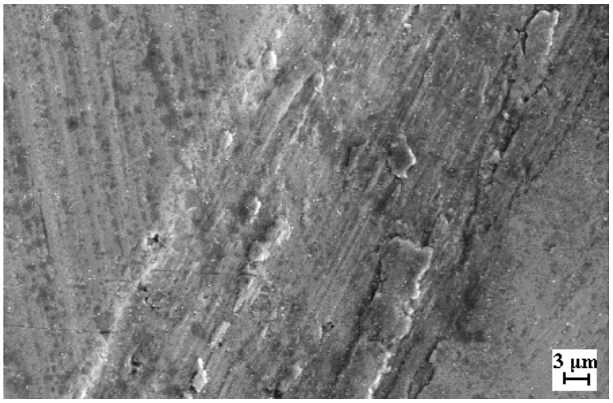

Fig. 8. SEM micrograph of the worn surface.

These preliminary tests therefore indicate that TiNi alloy specimens with the initial martensitic phase transformed to austenitic phase during wear process and this supports the basic claim in this work.

6. CONCLUSIONS

The high wear resistance of TiNi alloy has traditionally been attributed to its pseudoelastic nature alone but the present work indicates that the contact temperature rise due to frictional heat generated during sliding plays an important role. Based on Liang and Rogers [8] and others [21,22,25,29,30] works a simple theoretical model to relate the wear resistance of TiNi alloys to contact temperature rise during sliding against other materials has been proposed in equations (9) and (14). A realistic contact temperature model [29] for rough sliding bodies has been incorporated and the resulting wear model that takes into account multiple heat source at the sliding contact is proposed in equation (19). The model again predicts an increase in wear resistance with temperature.

Preliminary sliding tests were carried out with a near equi-atomic TiNi alloy both at (a) a constant load and speed combination but at varying specimen temperature and (b) a

constant load and ambient temperature but at varying sliding speed. In both cases wear level fell with the increase in temperature and the results agree well with the theoretical prediction. The results are of importance in industrial practice where contact temperature rise is considered to be detrimental to smooth sliding for most engineering materials whereas here it seems that the temperature rise may prove to be tribologically useful for TiNi alloys. However more work is needed to establish the range of temperature rise where the effect is of practical use.

NOMENCLATURE

a Contact radius,

a_A Material constant ($= C\pi/(A_f^0 - A_s^0)$),

A_f Austenitic phase finish temperature,

A_r Total real area of contact per unit area,

A_s Austenitic phase start temperature,

A^o_f Austenitic phase start temperature in stress free state,

A^o_s Austenitic phase finish temperature in stress free state,

B Material constant ($= A_s^o + \frac{\pi}{a_A}$),

c Specific heat,

C Constant,

E Elastic modulus,

E^* Equivalent elastic modulus,

$\bar{E}$ Non-dimensional elastic modulus,

H Hardness of the softer of the two rubbing material,

$\overline{H}$ Non-dimensional hardness,

K Thermal conductivity,

K_w Wear coefficient,

L Non-dimensional Speed Parameter,

M_f Martensitic phase finish temperature,

M_s Martensitic phase start temperature,

n Number of asperities in contact per unit area ,

N Total number of asperities per unit area,

P Normal Load,

r Asperity radius,

R Protrusion radius,

T Alloy specimen temperature,

T_{bulk} Bulk temperature,

$\bar{T}$ Non-dimensional temperature,

v Sliding Speed,

$\bar{v}_e$ Non-dimensional velocity in elastic case,

$\bar{v}_p$ Non-dimensional velocity in plastic case,

V Wear volume,

$\bar{V}$ Non-dimensional wear volume,

$\bar{V}_{avhe}$ Non-dimensional average wear volume for high speed elastic case,

$\bar{V}_{avhp}$ Non-dimensional average wear volume for high speed plastic case,

$\bar{V}_{avle}$ Non-dimensional average wear volume for low speed elastic case,

$\bar{V}_{avlp}$ Non-dimensional average wear volume for low speed plastic case,

W Normal load,

W_e Total elastic load per unit area,

W_p Total plastic load per unit area,

$\bar{W}$ Non-dimensional Load,

x Sliding distance,

μ Coefficient of friction,

ρ Density,

ξ Martensite volume fraction,

υ Poisson's ratio,

ψ Plasticity index,

$\varphi(z)$ Surface height distribution,

σ Standard deviation of the surface height distribution,

σ' Applied Stress,

$\bar{\sigma}$ Non-dimensional roughness,

θ Contact temperature rise,

θ_{avhe} Average flash temperature for high speed elastic case,

θ_{avhp} Average flash temperature for high speed plastic case,

θ_{avle} Average flash temperature for low speed elastic case,

θ_{avlp} Average flash temperature for low speed plastic case,

θ_{mhe} Mean contact temperature rise for high speed elastic case,

θ_{mhp} Mean contact temperature rise for high speed plastic case,

θ_{mLe} Mean contact temperature rise for low speed elastic case,

θ_{mlp} Mean contact temperature rise for low speed plastic case.

REFERENCES

[1] W.J. Buehler, J.W. Gilfrich, R.C. Wiley: *Effects of low-temperature phase changes on the mechanical properties of alloys near composition TiNi,* Journal of Applied Physics, Vol. 34, pp. 1475 -1477, 1963.

[2] F.E. Wang, W.J. Buehler, S.J. Pickart: *Crystal structure and a unique martensitic transition of TiNi,* Journal of Applied Physics, Vol. 36, pp. 3232-3239, 1965.

[3] J. Perkin: *Shape Memory Effects in Alloys*, Plenum Press, New York, 1976.

[4] S. Kajiwara: *Characteristic features of shape memory effect and related transformation behavior in Fe-based alloys*, Materials Science and Engineering, Vol. 273-275, pp. 67-88, 1999.

[5] C.M. Wayman: *Some Applications of Shape-Memory Alloy,* Journal of Metals, Vol. 32, pp. 129-137, 1980.

[6] W.R. Saunders, H.H. Robertsaw, C.A. Rogers: *Structural Acoustic Control of a Shape Memory Alloy Composite Beam,* Journal of Intelligent Material Systems and Structures, Vol. 2, No. 4, pp. 508 -527, 1991.

[7] K. Tanaka, R. Iwasaki: *A Phenomenological Theory of Transformation Superplasticity*, Engineering Fracture Mechanics, Vol. 21, No. 4, pp. 709-720, 1985.

[8] C. Liang, C.A. Rogers: *One-Dimensional Thermomechanical Constitutive Relations for Shape Memory Materials*, Journal of Intelligent Material Systems and Structures, Vol. 1, No. 2, pp. 207-234, 1990.

[9] P. Clayton: *Tribological behaviour of titanium-nickel alloy*, Wear, Vol. 162-164, pp. 202-210, 1993.

[10] D.Y. Li: *Exploration of NiTi SMA for potential application in a new area: Tribological engineering,* Journal of Smart Material Structures, Vol. 9, pp. 717-726, 2000.

[11] K.N. Melton, O. Mercier: *Fatigue of NiTi thermoelastic martensites*, Acta Metallurgica, Vol. 27, pp. 137-144, 1979.

[12] L.G. Korshunov, V.G. Pushin, N.L. Cherenkov, V.V. Makarov: *Structural transformations, strengthening, and wear resistance of titanium nickelide upon abrasive and adhesive wear*, The Physics of Metals and Metallography, Vol. 10, pp 91-101, 2010.

[13] S.K. Wu, H.C. Lin, C.H. Yeh: *A comparison of the cavitation erosion resistance of TiNi alloys SUS304 stainless steel and Ni-based self-fluxing alloy*, Wear, Vol. 244, pp. 85-93, 2000.

[14] Y. Shida, Y. Sugimoto: *Water jet erosion behavior of Ti-Ni binary alloys,* Wear, Vol. 146, pp. 219-228, 1991.

[15] I. Cvijović-Alagić, S. Mitrović, Z Cvijović, Đ. Veljović, M. Babić, M. Rakin: *Influence of the Heat Treatment on the Tribological Characteristics of the Ti-based Alloy for Biomedical Applications*, Tribology in Industry, Vol. 31, No. 3-4, pp. 17-22, 2009.

[16] A. Ball: *On the importance of work hardening in the design of wear resistant materials*, *Wear*, Vol. 91, pp. 201-207, 1983.

[17] T.W. Duerig, R. Zando: *Engineering Aspects of Shape Memory Alloys*, in: T.W. Duerig, K.N. Melton, D. Stockel, C.M. Wayman (Eds.): Butterworth Heinemann, London, pp. 369, 1990.

[18] S. Hattori, A. Tainaka: *Cavitation erosion of Ti-Ni base shape memory alloys*, Wear, Vol. 262, pp. 191-197, 2007.

[19] M. Abedini, H.M. Ghasemi, M. Nili Ahmadabadi: *Tribological behavior of NiTi alloy in martensitic and austenitic states*, Materials and Design, Vol. 30, pp. 4493– 4497, 2009.

[20] Linmao Qian, Qingping Sun, Xudong Xiao: *Role of phase transition in the unusual microwear behavior of superelastic NiTi shape memory alloy*, Wear, Vol. 260, pp. 509-522, 2006.

[21] K. Tanaka: *A Thermomechanical sketch of shape memory effect: one dimensional tensile behavior*, Res. Mechanica, Vol. 18, pp. 251-263, 1986.

[22] L.C. Brinson: *One Dimensional Constitutive Behavior of Shape Memory Alloys, thermomechanical derivation with non- constant material functions*, Journal of Intelligent Material Systems and Structures, Vol. 4, No. 2, pp. 229-242, 1993.

[23] H. Block: *General discussion on lubrication*, Proceeding of Institution of Mechanical Engineers, Vol. 2, pp. 222, 1937.

[24] J.C. Jaegar: *Moving sources of heat and the temperature at sliding surfaces*, Proceeding of Royal Society, N.S.W, Vol. 66, pp. 203–204, 1942.

[25] J.F. Archard: *The temperature of rubbing surfaces*, Wear, Vol. 2, pp. 438 - 455, 1959.

[26] B. Gecim, W.O. Winer: *Transient temperatures in the vicinity of an asperity contact*, *ASME J. Tribol.*, Vol. 107, pp. 333–342, 1985.

[27] R. Wolf: *The influence of surface roughness texture on the temperature and scuffing in sliding contact*, Wear, Vol. 143, pp. 99–117, 1990.

[28] S. Wang, K. Komvopoulos: *A fractal theory of the interfacial temperature distribution in the slow sliding regime: Part I—Elastic contact and heat*

Transfer analysis, ASME Journal of Tribology, Vol. 116, pp. 812– 823, 1994.

[29] D. Guha, S.K. Roy Chowdhury: *The effect of surface roughness on the temperature at the contact between sliding bodies*, Wear, Vol. 197, pp. 63-73, 1994.

[30] S.K. Roy Chowdhury, H.M. Pollock: *Adhesion between metal surfaces, The Effect of surface roughness*, Wear, Vol. 66, pp. 307-321, 1981.

[31] L.G Korshunov, V.G. Pushin, N.L. Cherenkov: *Effect of frictional heating on surface layer structure and tribological properties of titanium-nicklide*, Physics of Metals and Metallography, Vol. 112, pp. 290 – 300, 2011.